Journal of Sedimentary Research

Journal of Sedimentary Research, 2007, v. 77, 980–991
Research Article
DOI: 10.2110/jsr.2007.087

A REVIEW AND SYNTHESIS OF GLENDONITES (PSEUDOMORPHS AFTER IKAITE) WITH NEW DATA: ASSESSING APPLICABILITY AS RECORDERS OF ANCIENT COLDWATER CONDITIONS

BRUCE W. SELLECK,[1] PAUL F. CARR,[2] AND BRIAN G. JONES[2]
[1]*Department of Geology, Colgate University, Hamilton, New York 13346, U.S.A.*
[2]*School of Earth and Environmental Sciences, University of Wollongong, NSW, Australia, 2522*
e-mail: bselleck@mail.colgate.edu

ABSTRACT: **Calcite pseudomorphs after ikaite (glendonite) are associated with coldwater depositional systems, including glaciomarine and deepwater settings, as dictated by the limited stability field of ikaite. Ikaite precipitation is favored by elevated alkalinity and dissolved phosphate, conditions encountered commonly in association with organic-rich marine sediments where methane oxidation is occurring. The rapid recrystallization of ikaite to calcite during slight warming or pressure release results in considerable solid volume loss, producing a highly porous crystal mesh. Preservation of the original ikaite crystal form requires precipitation of diagenetic calcite cement during early burial to prevent compaction and collapse of pseudomorph structures. During later burial diagenesis remaining pore space may be filled with deeper burial calcite cement. Glendonites from the Permian of the Sydney Basin occur in subtidal shelf facies containing glacial dropstones and a normal marine fauna.**

Stable oxygen isotope signatures of modern ikaite suggest carbonate precipitation in equilibrium with ambient seawater; carbon signatures are usually strongly negative relative to normal marine carbonate, consistent with derivation of carbonate from methane oxidation. Review of published data suggests that while Holocene glendonite may provide reliable isotopic records of the conditions of ikaite precipitation, precipitation of later calcite cement within the glendonite structure reduces the significance of the isotopic signature as an indicator of primary depositional conditions. Bulk glendonite samples from the Permian Sydney Basin, Australia, have a broad range of $\delta^{18}O$ and $\delta^{13}C$ ($\delta^{18}O_{PDB} = -5$ to $-15‰$; $\delta^{13}C = -8$ to $-16‰$), in contrast to the narrow range for brachiopod carbonate ($\delta^{18}O_{PDB} = +1$ to $-5‰$; $\delta^{13}C = +5$ to $+7‰$) from the same strata. Handpicked separates of "primary" glendonite and secondary calcite also have a wide range of stable isotope values. The data from Sydney Basin glendonites indicate that diagenetic precipitation of calcite has blurred the isotopic signature of primary ikaite replacement calcite at the scale of micosampling done in this study.

INTRODUCTION

Precipitation of ikaite ($CaCO_3 \cdot 6H_2O$) in modern waters is limited by its stability field to near-freezing temperatures (Marland 1975), and is apparently favored by alkaline conditions and elevated phosphate concentrations. Widespread occurrence of ikaite in sediments of cold-climate shelves and estuaries, and in deeper ocean basins (Pauly 1963; Suess et al. 1982; Kennedy et al. 1987; Buchardt et al. 1998; Kodina et al. 2002) suggests that its formation is a relatively common phenomenon controlled largely by temperature and alkalinity. Occurrence of ikaite in lacustrine and terrestrial spring settings (Shearman and Smith 1985; Bischoff et al. 1993b; Council and Bennett 1993; Benson 1994; Ito 1996; Shearman 1998; Whiticar and Suess 1998) indicates that it can precipitate from a wide range of water chemistries. Ikaite crystals rapidly decompose to calcite plus water when warmed above 4°C (Bischoff et al. 1993a; Ito 1998; Koenigsberger et al. 1999). Although elevated levels of dissolved phosphorous may modestly increase the stability field of ikaite (Bischoff et al. 1993a) the relatively strict temperature limits on its stability make ikaite a robust indicator of cold water conditions and thus of great paleoclimatic significance when its former presence can be detected in ancient sediments. The stable-isotope characteristics of modern ikaite suggest that its fractionation factors are similar to those of calcite (Buchardt et al. 2001; Kodina et al. 2003), and thus it may reliably record seawater isotopic character given its narrow range of stability. The recent study by Rickaby et al. (2006) demonstrated that the fractionation factor for $\delta^{18}O$ between ikaite hydration water and seawater is 1.0029, and these authors concluded that ikaite is an optimal candidate for reconstructing the evolution of seawater $\delta^{18}O$.

The conversion of ikaite to calcite plus water may result in the generation of pseudomorphic calcite aggregates whose external form is controlled by the ikaite crystal morphology. The eminent mineralogist James Dwight Dana was presented with samples of these pseudomorphs from a property named "Glendon" (in the Hunter Valley, NSW, Australia) during his visit to the area in 1840 as part of the US Exploring Expedition. During the expedition he also collected specimens from the Astoria area, Oregon, and recognized the similarity between these samples and those from Glendon (Dana 1849). He concluded that the samples were pseudomorphs because of their granular interior, but he was unable to determine the identity of the precursor. These pseudomorphs were subsequently named glendonites by David et al. (1905) after the original locality, but many other names, including barley corns, chrysanthemum stones, fundylite, gennoishi, hedgehogs, jarrowite, opal pineapples, pseudogaylussite, thinolite, and White Sea hornlets, have also

 1527-1404/07/077-980/$03.00

TABLE 1.—*Location, stratigraphic, morphological and stable isotope data for analysed samples.*

Sample	Unit, location and facies	Age	Material analysed	$\delta^{13}C_{VPDB}$, ‰	$\delta^{18}O_{VPDB}$, ‰
MG-2a-blk	Kola Peninsula, Russia; estuarine	Late Neogene	outcrop sample; bulk glendonite	−15.63	−1.04
MG-2a-sh	Kola Peninsula, Russia; estuarine	Late Neogene	outcrop sample; bivalve shell	−0.87	−2.50
MG-1	Kola Peninsula, Russia; estuarine	Late Neogene	outcrop sample; bulk glendonite	−15.12	−0.99
OR	Alkali Lake, Oregon; lacustrine	Late Neogene	outcrop sample; bulk glendonite	5.78	−6.25
PYLK	Pyramid Lake, Nevada; lacustrine	Late Neogene	outcrop sample; bulk glendonite	2.86	−2.22
PS-7e	coarse spar in Westley Park Sandstone; Werri Beach, Sydney Basin; spar		bulk spar sample from sandy facies	−3.29	−12.94
WB-1	vein in Westley Park Sandstone; Werri Beach, Sydney Basin; vein		outcrop sample; bulk spar sample from vein ~ 5 m below Permian basalt flow	−0.94	−24.22
BT-2a-dk	Kulnura Marine Tongue, Illawarra Coal Measures, Diamond Drill Hole AGL Bootleg 2A, Sydney Basin; shallow marine	Permian	drill core sample from 1376.35 m depth; amber calcite separate from glendonite	−3.02	−13.57
BT-2a-lt	Kulnura Marine Tongue, Illawarra Coal Measures, Diamond Drill Hole AGL Bootleg 2A, Sydney Basin; shallow marine	Permian	drill core sample from 1376.35 m depth; clear calcite separate from glendonite	−2.44	−13.68
BT-2a-lt	Kulnura Marine Tongue, Illawarra Coal Measures, Diamond Drill Hole AGL Bootleg 2A, Sydney Basin; shallow marine	Permian	drill core sample from 1376.35 m depth; clear calcite separate from glendonite	−2.44	−13.68
GLEN-a	Mulbring Siltstone; Glendon, Sydney Basin; shallow marine	Permian	outcrop sample; bulk glendonite	−15.86	−6.98
GLEN-b	Mulbring Siltstone; Glendon, Sydney Basin, shallow marine	Permian	outcrop sample; bulk glendonite	−17.09	−6.80
WH-9a	Wandrawandian Siltstone; Huskisson, Sydney Basin; shallow marine	Permian	outcrop sample; brachiopod shell, *Spirifer* sp.	3.39	−3.34
WH-9b	Wandrawandian Siltstone; Huskisson, Sydney Basin; shallow marine	Permian	outcrop sample; brachiopod shell, *Spirifer* sp.	4.25	−4.91
WH2-Ba	Wandrawandian Siltstone; Huskisson, Sydney Basin; shallow marine	Permian	outcrop sample; brachiopod shell, *Spirifer* sp.	3.72	−2.68
WH2-Bb	Wandrawandian Siltstone; Huskisson, Sydney Basin; shallow marine	Permian	outcrop sample; brachiopod shell, *Spirifer* sp.	4.29	−4.51
WH-1b	Wandrawandian Siltstone; Huskisson, Sydney Basin; shallow marine	Permian	outcrop sample; bulk glendonite	−12.50	−7.78
KP-2b	Wandrawandian Siltstone; Kinghorn Point, Sydney Basin; shallow marine	Permian	outcrop sample; bulk glendonite	−13.30	−16.93
H3	Wandrawandian Siltstone; Huskisson, Sydney Basin; shallow marine	Permian	outcrop sample; bulk glendonite	−11.82	−9.50
H1-b	Wandrawandian Siltstone; Huskisson, Sydney Basin; shallow marine	Permian	outcrop sample; bulk glendonite	−9.00	−21.40
WH2-a	Wandrawandian Siltstone; Huskisson, Sydney Basin; shallow marine	Permian	outcrop sample; bulk glendonite	−13.53	−9.76
H4-a	Wandrawandian Siltstone; Huskisson, Sydney Basin; shallow marine	Permian	outcrop sample; bulk glendonite	−14.28	−8.13
KP-7b	Wandrawandian Siltstone; Kinghorn Point, Sydney Basin; shallow marine	Permian	outcrop sample; bulk glendonite	−16.35	−9.30
KP-7b-dk	Wandrawandian Siltstone; Kinghorn Point, Sydney Basin; shallow marine	Permian	outcrop sample; amber calcite separate from glendonite	−9.10	−13.40
KP-7b-lt	Wandrawandian Siltstone; Kinghorn Point, Sydney Basin; shallow marine	Permian	outcrop sample; clear calcite separate from glendonite	−14.04	−10.74
WH-7	Wandrawandian Siltstone, Huskisson, Sydney Basin; shallow marine	Permian	outcrop sample; bulk glendonite	−13.17	−5.18
WH-7-dk	Wandrawandian Siltstone, Huskisson, Sydney Basin; shallow marine	Permian	outcrop sample; amber calcite separate from glendonite	−12.46	−6.16
WH-7-lt	Wandrawandian Siltstone, Huskisson, Sydney Basin; shallow marine	Permian	outcrop sample; clear calcite separate from glendonite	−11.49	−6.86
WH-4	Wandrawandian Siltstone, Huskisson, Sydney Basin	Permian	outcrop sample; bulk glendonite	−12.92	−8.12
WH-4-dk	Wandrawandian Siltstone, Huskisson, Sydney Basin	Permian	outcrop sample; amber calcite separate from glendonite	−13.01	−10.53
WH-4-lt	Wandrawandian Siltstone, Huskisson, Sydney Basin; shallow marine	Permian	outcrop sample; clear calcite separate from glendonite	−13.11	−11.22
WH-ORG-1	Wandrawandian Siltstone; Warden Head, Sydney Basin, shallow marine	Permian	outcrop sample; coalified wood	−22.40	
WH-ORG-2	Wandrawandian Siltstone; Warden Head, Sydney Basin, shallow marine	Permian	outcrop sample; coalified wood	−21.70	
TUN543.3	Quamby Formation; Diamond Drill Hole Tunbridge RG145; Tasmania Basin, shallow marine	Permian	drill core sample from 543.3 m depth; bulk glendonite	−3.95	−7.55
TUN554.4	Quamby Formation; Diamond Drill Hole Tunbridge RG145; Tasmania Basin, shallow marine	Permian	drill core sample from 554.4 m depth; bulk glendonite	−2.43	−7.72
TUN541.7	Quamby Formation; Diamond Drill Hole Tunbridge RG145; Tasmania Basin, shallow marine	Permian	drill core sample from 541.7 m depth; bulk glendonite	−0.14	−6.76
TUN637-dk	Quamby Formation; Diamond Drill Hole Tunbridge RG145; Tasmania Basin, shallow marine	Permian	drill core sample from 637.0 m depth; amber calcite separate from glendonite	−8.71	−8.74
TUN637-lt	Quamby Formation; Diamond Drill Hole Tunbridge RG145; Tasmania Basin, shallow marine	Permian	drill core sample from depth 637.0 m; clear calcite separate from glendonite	−12.87	−8.38

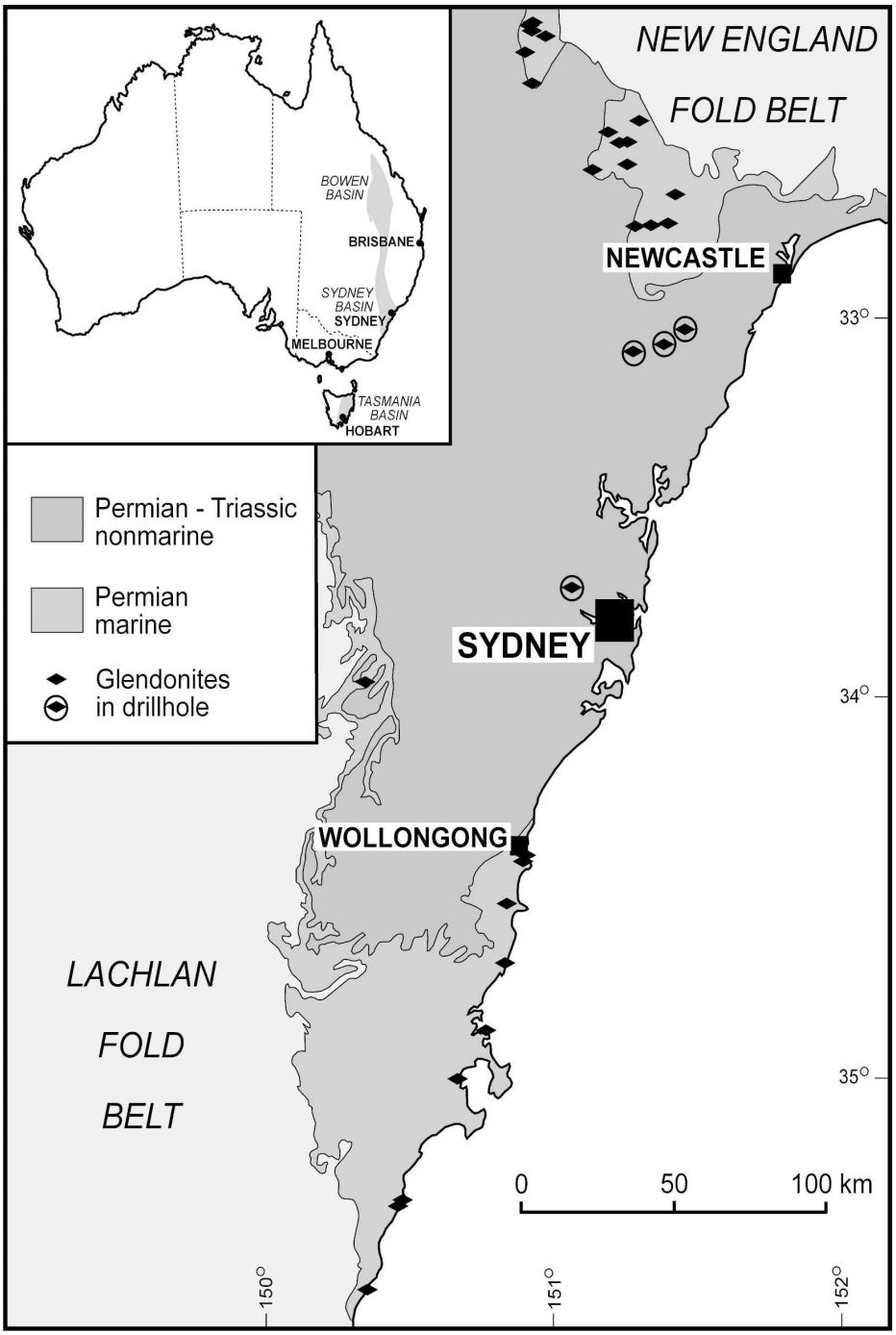

FIG. 1.—Location map showing generalized geology and glendonite localities in the Sydney Basin, New South Wales, Australia. Localities shown in nonmarine strata come from drill holes penetrating underlying marine units.

been used. Glendonites have been recognized from many localities in strata ranging from Precambrian (Johnston 1995; James et al. 2005) to Recent (Table 1). They are an important climate proxy and have been widely reported in association with coldwater sedimentary facies, often within glaciomarine settings (Brandt 1986; Francis and Frakes 1988; Sheard 1990; Brandley and Krause 1994; Bradshaw et al. 1995; Johnston 1995; Yan 1996; Shi 2001).

The formation of glendonite involves the rapid conversion of ikaite to calcite at temperatures above 4°C (Marland 1975; Swainson and Hammond 2001), and thus there is potential for using the stable-isotope characteristics of the calcite in glendonites that directly replaces ikaite as a recorder of water isotope chemistry in the depositional to early burial setting. Measured isotopic values for pseudomorphous calcite certainly appear to mimic the original ikaite isotopic values because ikaite samples that transformed to calcite at 20°C have the same O and C isotopic composition as those that were freeze dried at −56°C (Greinert and Derkachev 2004). The narrow range of temperature at which the conversion takes places limits the uncertainty involved in calculation of water isotopic chemistry based upon temperature-dependent fractionation factors, thus increasing the utility of glendonite calcite as a record of isotopic signatures of the precipitating fluid. In particular, the isotopic composition of glendonite calcite might be used to assess the reliability of biogenic carbonate in recording seawater composition and/or temperature (De Lurio and Frakes 1999). Given the uncertain reliability with

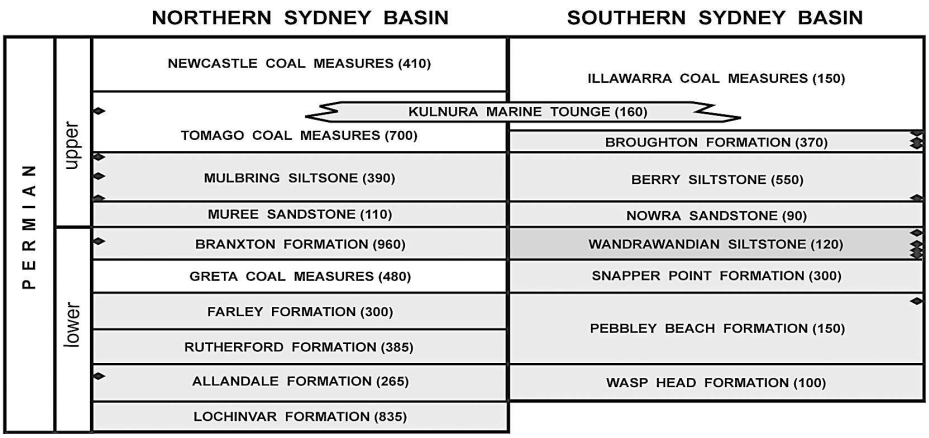

FIG. 2.—Generalized stratigraphy of Permian strata in the Sydney Basin. Stratigraphic position of glendonite-bearing horizons is indicated by diamond symbol.

which some biogenic carbonate records the primary isotopic signature of seawater (Veizer et al. 1999; Auclair et al. 2003; Brand 2004), availability of another primary seawater chemistry proxy would be of considerable value in refining the long-term trends in evolution of Phanerozoic seawater (Veizer et al. 1999). Conversion of ikaite to calcite, however, involves a volume decrease of approximately one-third, resulting in development of high porosity within a loose mesh or "cage" of calcite crystals. Later precipitation of void-filling calcite may occur under physical and chemical conditions that are very different from the original depositional setting. This, of course, limits the reliability of stable-isotope results unless the primary calcite phase that was formed from ikaite conversion can be identified and analyzed.

In the current paper we examine the depositional environments and sedimentary petrology of glendonites in the Permian strata of eastern Australia (Figs. 1, 2) and report the results of stable-isotope analysis of glendonite calcite and associated biogenic carbonate. Additional results from a sampling of nonmarine, Quaternary glendonite occurrences are presented. We also review published isotopic data on ikaite and glendonite calcite to assess the reliability of glendonites as climate proxies and as records of stable-isotope chemistry of waters in the depositional setting.

Glendonite Presursor

The identity of the precursor mineral to glendonites has been the subject of considerable debate since the publication of the first description of these pseudomorphs by Dana (1849). A wide range of minerals, including anhydrite ($CaSO_4$), aragonite ($CaCO_3$), celestite ($SrSO_4$), gaylussite ($CaCO_3{\cdot}Na_2CO_3{\cdot}5H_2O$), glauberite ($Na_2SO_4{\cdot}CaSO_4$), gypsum ($CaSO_4{\cdot}2H_2O$), natron ($Na_2CO_3{\cdot}10H_2O$), pirssonite ($CaCO_3{\cdot}Na_2CO_3{\cdot}5H_2O$), sulfur (S), thenardite (Na_2SO_4), thermonatrite ($Na_2CO_3{\cdot}H_2O$), weddellitte ($CaC_2O_4{\cdot}2H_2O$), and whewellite ($CaC_2O_4{\cdot}H_2O$) have been suggested as possible precursors, with glauberite and thenardite probably being the most favored choices.

Synthetically produced calcium carbonate hexahydrate ($CaCO_3{\cdot}6H_2O$) had been known to chemists before James Dana visited the Hunter Valley and described the original glendonites, but it was not found in nature until more than a century later when the mineral ikaite was discovered in the very cold waters of Ikka Fjord, southern Greenland (Pauly 1963). This discovery provided the first indication of the identity of the elusive precursor mineral and also vindicated the suspicions held by at least some mineralogists more than a century ago. According to Edward Dana, who investigated the "thinolites" from Lake Lahontan, Nevada, "the original mineral was one which does not appear thus far to have been observed in its natural condition, although, as will be shown later, it probably has occurred abundantly at numerous other localities" (Dana 1884). Following the discovery of ikaite it took nearly another two decades before Kaplan (1979) recognized that the composition, morphology, and distribution of this new mineral matched those required for the precursor to glendonites. Ironically, Boggs (1972) had considered calcium carbonate hexahydrate as a potential precursor for Miocene glendonites from Astoria, Oregon, but he rejected it because he was not convinced that glendonites had monoclinic symmetry. Ikaite has now received widespread acceptance as the precursor mineral for glendonites and related pseudomorphs (e.g., Suess et al. 1982; Carr et al. 1989; Swainson and Hammond 2001).

Whether the ikaite-to-calcite transformation is a single-stage process or involves one or more intermediate compounds is equivocal. Stein and Smith (1986) noted that ikaite samples recovered during drilling in the Nankai Trough transformed to mixtures of aragonite and calcite, and finally calcite after opening the drill cores. The common occurrence of monohydrocalcite ($CaCO_3{\cdot}H_2O$) with ikaite in Ikka Fjord may reflect its formation as an intermediate phase, but this phase was not detected by Buchardt et al. (2001) during recrystallization of ikaite to calcite in the laboratory. The rare mineral vaterite (hexagonal $CaCO_3$) has also been recognized as an intermediate phase during decomposition of synthetic ikaite at room temperature (Shaikh and Shearman 1987; Lennie et al. 2004). Both monohydrocalcite and vaterite have been recorded as decomposition products after ikaite in the Hokkaido spring, Japan (Ito et al. 1999).

Ikaite and Glendonite Occurrences

Tables 1 and 2 present a compilation of ikaite and glendonite occurrences. In the last two decades ikaite has been recognized from around the globe in a wide array of facies ranging from springs and lakes to estuaries, shallow-marine shelves, and deep oceanic basins and troughs. All occurrences, however, are characterized by cold, alkaline conditions and, for at least some occurrences, elevated phosphate concentrations in precipitating waters. These elevated phosphate levels apparently suppress precipitation of calcite and aragonite (Buchardt et al. 2001). In contrast to aragonite and calcite, ikaite becomes increasingly insoluble with decreasing temperature (Bischoff et al. 1993a). In addition to these natural occurrences, the white spots formed in the shells of frozen shrimp (prawns) have also been identified as ikaite (Mikkelsen et al. 1999). Possible extraterrestrial occurrences include Mars, where an ancient, cold, alkali-rich ocean is postulated to have been conducive to the formation of ikaite (Socki et al. 2003).

Naturally formed ikaite occurs in two major forms comprising tufa associated with spring discharge, and crystals that grow within the sediment pile. Ikaite tufa deposits precipitate either directly from

TABLE 2.—*Stable-isotope analyses of glendonite and transformed ikaite.*

Location	Material	Age	Setting/Origin	$\delta^{13}C_{VPDB}$, ‰	$\delta^{18}O_{VPDB}$, ‰	Reference
Bowen Basin, Australia	glendonite	Permian	shallow marine	−20.2	−5.3	Huggett et al. 2005
Bowen Basin, Australia	glendonite	Permian	shallow marine	−13.6	−13.0	Huggett et al. 2005
Bowen Basin, Australia	glendonite	Permian	shallow marine	−15.1	−9.6	Huggett et al. 2005
Eromanga Basin, Australia	glendonite	Cretaceous	shallow marine	−15.02	0.0	De Lurio & Frakes 1999
Eromanga Basin, Australia	glendonite	Cretaceous	shallow marine	−21.76	−0.93	De Lurio & Frakes 1999
Eromanga Basin, Australia	glendonite	Cretaceous	shallow marine	−20.52	−1.12	De Lurio & Frakes 1999
Eromanga Basin, Australia	glendonite	Cretaceous	shallow marine	−14.51	−0.18	De Lurio & Frakes 1999
Eromanga Basin, Australia	glendonite	Cretaceous	shallow marine	−16.49	−1.62	De Lurio & Frakes 1999
Denmark	glendonite	Eocene		−25.2	−1.20	Huggett et al. 2005
Denmark	glendonite	Eocene		−21.2	−0.8	Huggett et al. 2005
Astoria, Oregon	glendonite	Miocene	shallow marine	−5.25	−10.87	Boggs 1972
Astoria, Oregon	glendonite	Miocene	shallow marine	−9.36	−7.07	Boggs 1972
Astoria, Oregon	glendonite	Miocene	shallow marine	−7.81	−9.01	Boggs 1972
Astoria, Oregon	glendonite	Miocene	shallow marine	−3.59	−9.58	Boggs 1972
Olympic Peninsula, Washington	glendonite	Tertiary	shallow marine	−6.5	−11.5	Whiticar & Suess 1998
Olympic Peninsula, Washington	glendonite	Tertiary	shallow marine	−5.2	−11.6	Whiticar & Suess 1998
Olympic Peninsula, Washington	glendonite	Tertiary	shallow marine	−4.8	−11.4	Whiticar & Suess 1998
Olympic Peninsula, Washington	glendonite	Tertiary	shallow marine	−4.6	−11.6	Whiticar & Suess 1998
Spitzbergen	glendonite	Tertiary	shallow marine	−15.7	−2.0	Whiticar & Suess 1998
Spitzbergen	glendonite	Tertiary	shallow marine	−13.5	−3.1	Whiticar & Suess 1998
Spitzbergen	glendonite	Tertiary	shallow marine	−11.1	−4.7	Whiticar & Suess 1998
Pyramid Lake, Nevada	thinolite	Late Neogene	lacustrine; springs	3.6	−1.6	Whiticar & Suess 1998
Pyramid Lake, Nevada	thinolite	Late Neogene	lacustrine; springs	3.4	−2.5	Whiticar & Suess 1998
Pyramid Lake, Nevada	thinolite	Late Neogene	lacustrine; springs	3.2	−2.6	Whiticar & Suess 1998
Pyramid Lake, Nevada	thinolite	Late Neogene	lacustrine; springs	3.3	−2.5	Whiticar & Suess 1998
Mono Lake, California	thinolite	Late Neogene	lacustrine; springs	4.3	−4.6	Whiticar & Suess 1998
Mono Lake, California	thinolite	Late Neogene	lacustrine; springs	4.3	−4.4	Whiticar & Suess 1998
Mono Lake, California	tufa	Late Neogene	lacustrine; springs	4.1	−4.3	Whiticar & Suess 1998
Mono Lake, California	thinolite	Late Neogene	lacustrine; springs	4.5	−1.9	Whiticar & Suess 1998
Mono Lake, California	thinolite	Late Neogene	lacustrine; springs	4.6	−1.9	Whiticar & Suess 1998
Arctic Canada	glendonite	Recent		−17.2	−7.0	Whiticar & Suess 1998
Arctic Canada	glendonite	Recent		−17.4	−5.9	Whiticar & Suess 1998
Arctic Canada	glendonite	Recent		−18.2	−5.2	Whiticar & Suess 1998
Arctic Alaska	ikaite	Recent		−19.9	−9.8	Whiticar & Suess 1998
Hokkaido Island, Japan	gennoishi	Recent	lacustrine	−0.8	−6.0	Whiticar & Suess 1998
River Tyne, England	jarrowite	Recent	estuarine	−28.5	−0.4	Whiticar & Suess 1998
River Tyne, England	jarrowite	Recent	estuarine	−27.0	−0.6	Whiticar & Suess 1998
Sea of Othotsk	glendonite	Recent	marine ~ 380 m	−19.0	3.7	Greinert & Derkachev 2004
Sea of Othotsk	glendonite	Recent	marine ~ 380 m	−21.0	3.6	Greinert & Derkachev 2004
Sea of Othotsk	glendonite	Recent	marine ~ 380 m	−21.0	3.8	Greinert & Derkachev 2004
Sea of Othotsk	glendonite	Recent	marine ~ 380 m	−24.0	3.6	Greinert & Derkachev 2004
Sea of Othotsk	glendonite	Recent	marine ~ 380 m	−24.5	3.75	Greinert & Derkachev 2004
Sea of Othotsk	glendonite	Recent	marine ~ 380 m	−24.5	4.05	Greinert & Derkachev 2004
Sea of Othotsk	glendonite	Recent	marine ~ 380 m	−25.0	3.7	Greinert & Derkachev 2004
Sea of Othotsk	glendonite	Recent	marine ~ 380 m	−25.5	3.75	Greinert & Derkachev 2004
Sea of Othotsk	glendonite	Recent	marine ~ 380 m	−26.0	3.7	Greinert & Derkachev 2004
Sea of Othotsk	glendonite	Recent	marine ~ 380 m	−26.5	3.7	Greinert & Derkachev 2004
Sea of Othotsk	glendonite	Recent	marine ~ 380 m	−27.0	4.2	Greinert & Derkachev 2004
Sea of Othotsk	glendonite	Recent	marine ~ 380 m	−27.5	3.95	Greinert & Derkachev 2004
Sea of Othotsk	glendonite	Recent	marine ~ 380 m	−29.5	4	Greinert & Derkachev 2004
Sea of Othotsk	glendonite	Recent	marine ~ 380 m	−31.5	3.75	Greinert & Derkachev 2004
Sea of Othotsk	glendonite	Recent	marine ~ 380 m	−33.5	3.5	Greinert & Derkachev 2004
Sea of Othotsk	transformed ikaite	Recent	marine ~ 380 m	−20.5	2.7	Greinert & Derkachev 2004
Sea of Othotsk	transformed ikaite	Recent	marine ~ 380 m	−21	2.85	Greinert & Derkachev 2004
Sea of Othotsk	transformed ikaite	Recent	marine ~ 380 m	−21.5	2.8	Greinert & Derkachev 2004
Sea of Othotsk	transformed ikaite	Recent	marine ~ 380 m	−21.5	2.95	Greinert & Derkachev 2004
Sea of Othotsk	transformed ikaite	Recent	marine ~ 380 m	−22.00	2.95	Greinert & Derkachev 2004
Sea of Othotsk	transformed ikaite	Recent	marine ~ 380 m	−21.50	3.05	Greinert & Derkachev 2004
Sea of Othotsk	transformed ikaite	Recent	marine ~ 380 m	−21.50	3.20	Greinert & Derkachev 2004
Sea of Othotsk	transformed ikaite	Recent	marine ~ 380 m	−21.00	2.85	Greinert & Derkachev 2004
Sea of Othotsk	transformed ikaite	Recent	marine ~ 380 m	−20.50	3.00	Greinert & Derkachev 2004
Sea of Othotsk	transformed ikaite	Recent	marine ~ 380 m	−22.50	2.70	Greinert & Derkachev 2004
Sea of Othotsk	transformed ikaite	Recent	marine ~ 380 m	−23.00	2.70	Greinert & Derkachev 2004
Sea of Othotsk	transformed ikaite	Recent	marine ~ 380 m	−22.00	2.90	Greinert & Derkachev 2004
Sea of Othotsk	transformed ikaite	Recent	marine ~ 380 m	−22.50	3.10	Greinert & Derkachev 2004
Zaire Fan	transformed ikaite	Recent	deep marine	−28.92	1.99	Jansen et al. 1987
Zaire Fan	transformed ikaite	Recent	deep marine	−25.52	2.72	Jansen et al. 1987
Zaire Fan	transformed ikaite	Recent	deep marine	−33.92	2.90	Jansen et al. 1987

TABLE 2.—Continued.

Location	Material	Age	Setting/Origin	$\delta^{13}C_{VPDB}$, ‰	$\delta^{18}O_{VPDB}$, ‰	Reference
Zaire Fan	transformed ikaite	Recent	deep marine	−32.52	2.75	Jansen et al. 1987
Zaire Fan	transformed ikaite	Recent	deep marine	−31.50	2.85	Zabel & Schultz 2001
Zaire Fan	transformed ikaite	Recent	deep marine	−29.60	3.02	Zabel & Schultz 2001
Zaire Fan	transformed ikaite	Recent	deep marine	−27.60	2.87	Zabel & Schultz 2001
Zaire Fan	transformed ikaite	Recent	deep marine	−26.70	3.06	Zabel & Schultz 2001
Zaire Fan	transformed ikaite	Recent	deep marine	−28.70	2.97	Zabel & Schultz 2001
Nankai Trough	transformed ikaite	Recent	deep marine	−28.88	2.93	Stein & Smith 1986
Nankai Trough	transformed ikaite	Recent	deep marine	−25.26	2.77	Stein & Smith 1986
Nankai Trough	transformed ikaite	Recent	deep marine	−30.41	3.12	Stein & Smith 1986
Nankai Trough	transformed ikaite	Recent	deep marine	−26.13	2.65	Stein & Smith 1986
Nankai Trough	transformed ikaite	Recent	deep marine	−28.06	2.88	Stein & Smith 1986
Nankai Trough	transformed ikaite	Recent	deep marine	−29.24	2.23	Stein & Smith 1986
Nankai Trough	transformed ikaite	Recent	deep marine	−31.42	2.54	Stein & Smith 1986
Nankai Trough	transformed ikaite	Recent	deep marine	−28.48	2.27	Stein & Smith 1986
Bransfield Strait	transformed ikaite	Recent	deep marine	−22.88	3.38	Suess et al. 1982
Bransfield Strait	transformed ikaite	Recent	deep marine	−18.79	3.84	Suess et al. 1982
Bransfield Strait	transformed ikaite	Recent	deep marine	−22.21	2.08	Suess et al. 1982
Bransfield Strait	transformed ikaite	Recent	deep marine	−18.94	0.95	Suess et al. 1982
Ikka Fjord	transformed ikaite	Recent	shallow marine; springs	−6.60	−8.75	Buchardt et al. 2001
Ikka Fjord	transformed ikaite	Recent	shallow marine; springs	−6.60	−9.35	Buchardt et al. 2001
Ikka Fjord	transformed ikaite	Recent	shallow marine; springs	−7.10	−12.25	Buchardt et al. 2001
Ikka Fjord	transformed ikaite	Recent	shallow marine; springs	−6.75	−9.30	Buchardt et al. 2001
Ikka Fjord	transformed ikaite	Recent	shallow marine; springs	−5.75	−10.10	Buchardt et al. 2001
Ikka Fjord	transformed ikaite	Recent	shallow marine; springs	−6.00	−9.90	Buchardt et al. 2001
Ikka Fjord	transformed ikaite	Recent	shallow marine; springs	−6.1	−9.9	Buchardt et al. 2001
Ikka Fjord	transformed ikaite	Recent	shallow marine; springs	−6.05	−10.2	Buchardt et al. 2001
Ikka Fjord	transformed ikaite	Recent	shallow marine; springs	−5.95	−10.5	Buchardt et al. 2001
Ikka Fjord	transformed ikaite	Recent	shallow marine; springs	−5.95	−10.75	Buchardt et al. 2001
Ikka Fjord	transformed ikaite	Recent	shallow marine; springs	−6.15	−10.45	Buchardt et al. 2001
Ikka Fjord	transformed ikaite	Recent	shallow marine; springs	−6.25	−10.3	Buchardt et al. 2001
Ikka Fjord	transformed ikaite	Recent	shallow marine; springs	−6.35	−10.35	Buchardt et al. 2001
Ikka Fjord	transformed ikaite	Recent	shallow marine; springs	−6.35	−10.45	Buchardt et al. 2001
Ikka Fjord	transformed ikaite	Recent	shallow marine; springs	−6.2	−11	Buchardt et al. 2001
Ikka Fjord	transformed ikaite	Recent	shallow marine; springs	−6.4	−10.95	Buchardt et al. 2001
Ikka Fjord	transformed ikaite	Recent	Shallow marine; springs	−6.45	−11	Buchardt et al. 2001
Ikka Fjord	transformed ikaite	Recent	shallow marine; springs	−6.35	−11.25	Buchardt et al. 2001
Ikka Fjord	transformed ikaite	Recent	shallow marine; springs	−6.25	−11.5	Buchardt et al. 2001
Laptev Sea	ikaite	Recent		−36.3	1.77	Schubert et al.1997

subaerially exposed springs (e.g., Hokkaido, Japan; Ito 1996, 1998) or, more commonly, during mixing associated with subaequeous discharge of springs in a submarine (e.g., Ikka Fjord, Greenland; Buchardt et al. 2001) or sublacustrine (e.g., Mono Lake, California; Bischoff et al. 1993b; Council and Bennett 1993) setting. Given the restricted temperature stability of the mineral, ikaite tufa may be ephemeral in many seasonal, cold-climate settings and be unrecognized in many localities. Recognition of such tufas in the geological record would be difficult, and we are unaware of any publication describing these features in pre-Quaternary sequences.

Ikaite also occurs as single crystals or groups, commonly as stellate clusters, that grow displacively within the sediment pile. Individual ikaite crystals seldom exceed a few centimeters in maximum dimension but single glendonite crystals range up to $>$ 1 m in length, and are commonly 5 to 15 cm long and 2 to 3 cm across the diagonal of rhomboid cross sections (Fig. 3A). Stellate glendonite clusters range up to $\sim$ 15 cm in diameter (Fig. 3B). Glendonites and related pseudomorphs are recognized in a wide range of geographic locations and in strata ranging from Precambrian (Johnston 1995) to Recent in age (Tables 1, 2). Geographic, stratigraphic, and morphological data for samples analyzed in the current study are summarized in Table 1.

Sydney Basin

The Sydney Basin of southeastern Australia consists of almost flat-lying, relatively undeformed Upper Carboniferous to Triassic marine and nonmarine strata and volumetrically minor igneous rocks (Fig. 1). The basin forms the southern part of the extensive, contiguous Sydney–Gunnedah–Bowen Basin, which developed initially as a failed rift (Fielding et al. 2001) followed by accumulation on the western margin of an elongate seaway that later developed into a foreland basin along the southeastern margin of Gondwana during the late Paleozoic and early Mesozoic. At that time, the region of the Sydney Basin was at high latitude, and basinal strata contain abundant evidence for very cold conditions (David et al. 1905; Gostin and Herbert 1973). Recent reevaluations of the late Paleozoic stratigraphic record of the Gondwanan ice age in eastern Australia (Dickens 1996; Tye et al. 1996; Eyles et al. 1998; Eyles and Eyles 2000; Isbell et al. 2003; Jones and Fielding 2004; Fielding et al. 2006) have suggested that three main glacial (icehouse) periods may have occurred between the mid-Carboniferous and the Early Permian. Glendonites are common in the Sydney Basin and have been recorded from more than 30 separate geographic localities (Carr et al. 1989) that represent six major glendonite-forming intervals; the Allandale Formation, the upper Pebbley Beach Formation, the Wandrawandian Siltstone and the Branxton Formation, the Berry–Mulbring Siltstones, the Broughton Formation, and the Kulnura Marine Tongue in the lower Illawarra Coal Measures (Fig. 2). All glendonite occurrences in the Sydney Basin have several features in common. In particular, all occur in dark gray, carbonaceous, Permian marine strata. The glendonites are restricted to particular stratigraphic intervals within each formation and tend to occur in several glendonite-bearing horizons within a stratigraphic

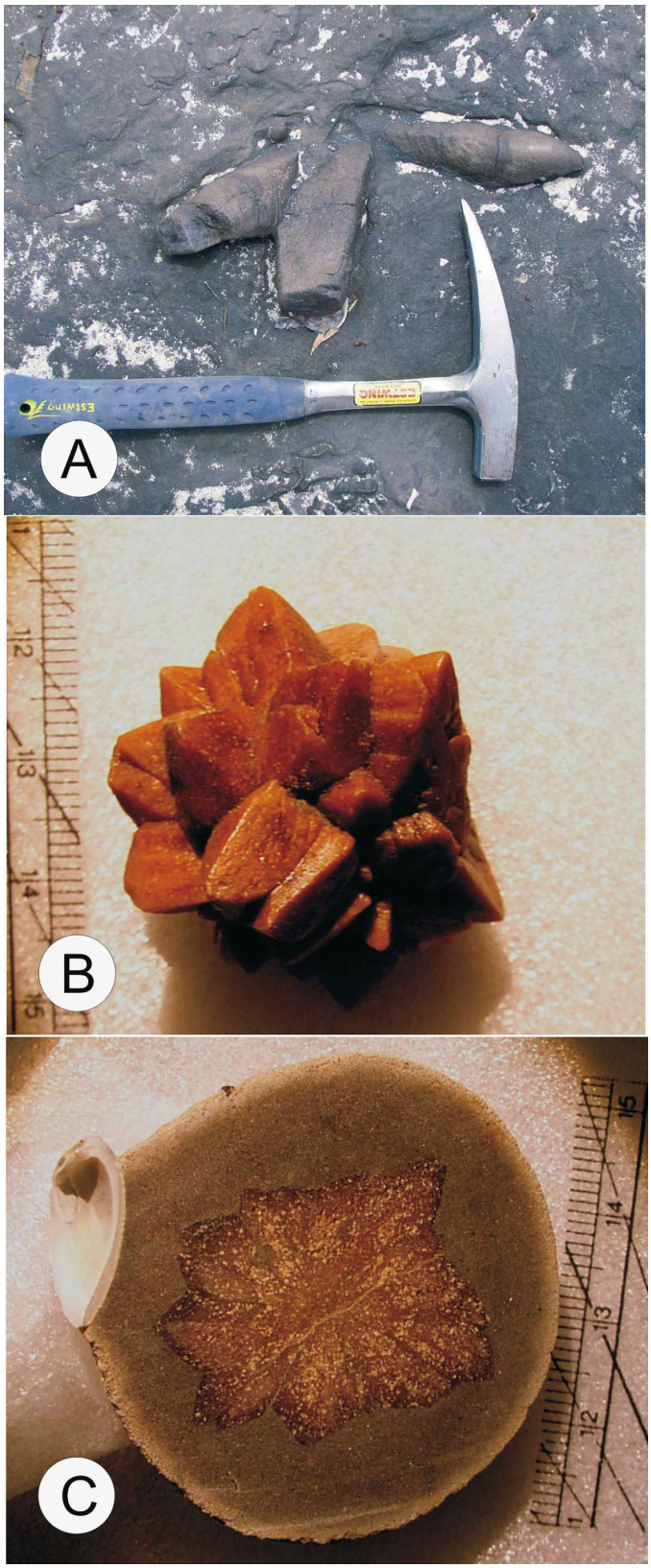

FIG. 3.—**A)** Stellate cluster of large glendonite pseudomorphs in the Wandrawandian Siltstone, Sydney Basin, New South Wales. **B)** "Pineapple" glendonite crystal array, Kola Peninsula. Scale in mm and cm.; **C)** Porous glendonite crystal array within concretion, Kola Peninsula. Note bivalve shell cemented within concretion. Scale in mm and cm.

interval several tens of meters thick. These horizons are composed of mudstone, siltstone, or rarely, very fine-grained sandstone that is commonly bioturbated. The glendonites are prismatic or stellate with randomly oriented long axes (Fig. 3A), and may partially or completely enclose fossils or pebbles. Glendonite-bearing beds are commonly overlain by sandy and/or fossiliferous beds that contain abundant rounded and less common subangular dropstones.

The glendonite-bearing formations are predominantly very fine-grained and represent periods of slow deposition where water depths were below storm wave base on an open continental shelf (lower three intervals) or in a protected seaway (upper three intervals). Between the glendonite-bearing formations coarser sand-dominated successions represent shallower-water offshore and shoreface facies (e.g., Le Roux and Jones 1994; Herbert 1995; Tye et al. 1996). The presence of glendonites in the Pebbley Beach Formation (and possibly in the Allandale Formation) may represent deposition under icehouse conditions during the last major phase of Gondwanan glaciation (Fielding et al. 2006). The relatively common occurrence of glendonites through the upper part of the Sydney Basin marine succession, however, indicates that cold conditions ($< 4^{\circ}C$) must have persisted at least periodically through most of the mid to Late Permian to allow the growth of ikaite crystals. Cold conditions with seasonal ice are also indicated throughout this succession by the presence of rounded erratic dropstones. Most of the formations (including the icehouse Pebbley Beach Formation) also contain wood fragments that have been washed into, and preserved in, the cold marine waters, thus indicating that the adjacent landmass supported a woody flora and the climate must have been only seasonally cold. The occurrence of glendonites in the deeper-water phases of Sydney Basin deposition is probably the result of tectonic downwarping of the basin rather than glacio-eustatic sea-level changes that would suggest that they formed during interglacial periods.

Petrology of Glendonites and Associated Sediments

The microscopic texture and fabric of glendonites from the Permian Sydney and Tasmanian Basins consist of brown to amber, blocky calcite crystals (2–50 microns) that form diffuse agglomerations and more regular dendritic arrays. These crystals contain minor micron-scale pyrite spherules and flecks of organic matter (Fig. 4A, B). The amber to brown calcite is interpreted as the calcite that formed during the early conversion of ikaite to calcite (Greinert and Derkachev 2004). Pore space within the brown to amber calcite network is filled with clear, coarsely crystallized secondary calcite cement. Calcite-filled pores range in size from millimeter to micron scale (Fig. 4B). Bioclasts are often included within glendonite crystals (Fig. 4C), but siliciclastic sediment from the surrounding mudstones is not (Fig. 4A). This suggests that the displacive growth of the ikaite excluded noncarbonate material or that ikaite preferentially nucleated in bioclast-rich zones. As noted below, sampling of glendonite for isotopic analyses attempted to distinguish amber-brown calcite, interpreted as most likely representing early replacement of ikaite, from clear or white calcite, interpreted as burial diagenetic cement.

Mudstone in a 1–15 cm zone surrounding a glendonite is often more tightly cemented by blocky calcite microspar, forming obvious concretionary masses cored by glendonite. Organic laminae and bioclasts are less compacted in this concretionary material than in adjacent sediment, suggesting development of the concretionary masses shortly after burial, and likely associated in time with the conversion of ikaite to calcite. Phosphatic conularids, minor phosphatization of bioclasts, and discrete phosphate clasts are common in the associated siliclastic sediment (Fig. 4D). In general, brachiopods from concretionary material adjacent to glendonites are well-preserved, with apparently minimal recrystallization and loss of primary microfabric (Fig. 4D).

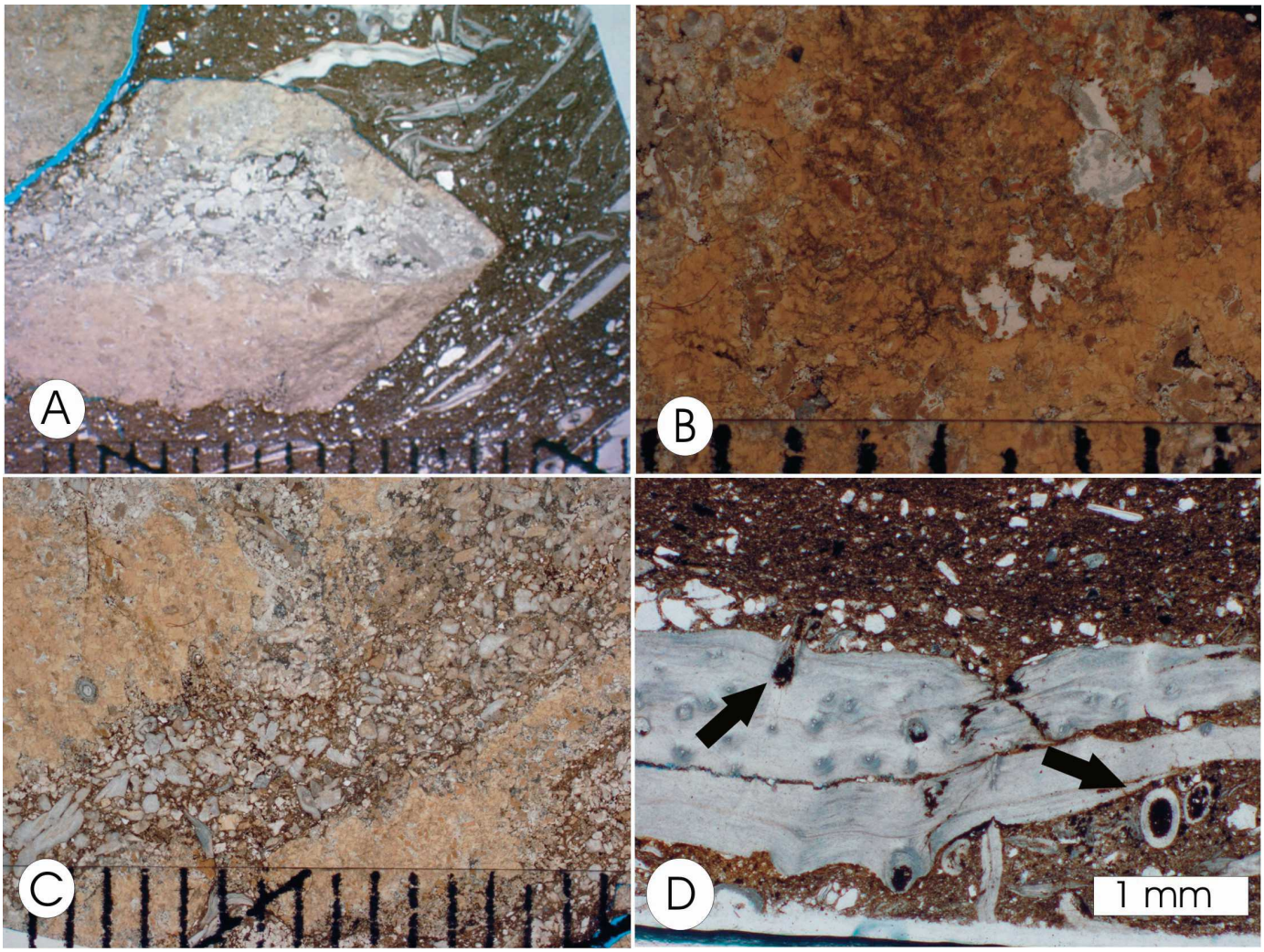

FIG. 4.—Photomicrographs (plane light) of glendonite and associated sediment. Wandrawandian Siltstone, Sydney Basin, NSW. **A)** Section of glendonite illustrating displacive growth of original ikaite crystal. Note abundant bioclasts. Scale in mm. **B)** Interior of glendonite illustrating darker (amber-brown) calcite with lighter clear-white calcite cement. Scale in mm. **C)** Glendonite with included bioclasts. Scale in mm. **D)** Bioclastic siltstone. Note Ca-phosphate infill of spines and punctae (arrows).

Joints within the glendonite-bearing units of the Shoalhaven Group in the southern Sydney Basin are mineralized with minor calcite and rare quartz. This mineralization is pervasive, and is likely related to later tectonic or burial phenomena. Some mineralized joints, however, may be related to hydrothermal fluid systems developed during emplacement of Late Permian basalts (Carr et al. 1999).

Stable Isotopes

Samples and Methods.—Stable-isotope analyses were carried out on glendonite samples from the Permian strata of the Sydney and Tasmania Basins (Domack et al 1998) of eastern Australia, and Quaternary units in the Kola Peninsula (Russia), Alkali Lake (Oregon), and Pyramid Lake (Nevada). In addition, shell material from the concretionary sediment surrounding Sydney Basin and Kola Peninsula glendonites, and two samples of calcite spar from mineralized joints in the Sydney Basin, were analyzed. Two samples of coalified wood from a Sydney Basin glendonite-bearing horizon were also analyzed for $\delta^{13}C$ to provide an indication of the isotopic composition of nonmarine organic material in the Permian glendonite-bearing strata.

Samples of glendonite, shell, and calcite spar were crushed to sand size, and separates were hand-picked under a binocular microscope. Picked separates were ground to $<$ 230 mesh and roasted at 300°C for one hour to remove organic carbon inclusions. Prepared samples were analyzed for carbon and oxygen and carbon SIRA at the Stable Isotope laboratory at New York State University at Albany. The samples were placed in septum vials and loaded into a heated rack with temperature controlled to $\pm$ 0.1°C. 100% phosphoric acid was sequentially needle injected producing CO_2 which was then passed to a Micromass Optimagas-source triple-collector mass spectrometer for determination of stable isotope ratios. Regular standardization with NBS-7 and replicate analysis of samples indicate precision of better than 0.1‰ for both $\delta^{13}C$ and $\delta^{18}O$. All isotopic data are reported relative to VPDB.

Results.—The results of the analyses are reported in Table 1 and are shown graphically as Figure 5. The Sydney Basin brachiopods (*Spirifer* sp.) form a relatively tight cluster with $\delta^{13}C \sim +3$ to +6‰ and $\delta^{18}O \sim +1$ to −4‰. These lie well within the range of stable-isotope compositions for Permian biogenic low-magnesium calcite reported in numerous studies as summarized by Veizer et al. (1999), and the recent

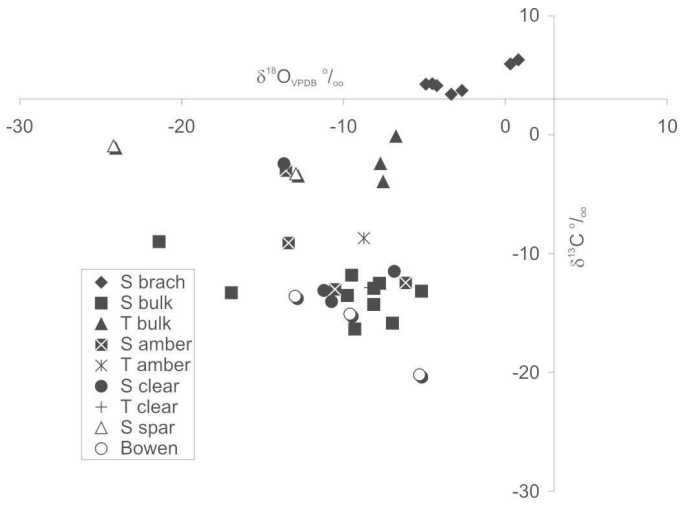

FIG. 5.—Stable-isotope data plot of glendonite calcite and related materials. S brach = brachiopods from Sydney Basin strata containing glendonites; S bulk = Sydney Basin bulk glendonite calcite; T bulk = Tasmania Basin bulk glendonite calcite; S amber = Sydney Basin glendonite amber-brown calcite handpicked separate; T amber = Tasmania Basin glendonite amber-brown calcite handpicked separate; S clear = Sydney Basin glendonite clear-white calcite handpicked separate; T clear = Tasmania Basin glendonite clear-white calcite handpicked separate; S spar = Sydney Basin hydrothermal calcite; Bowen = Bowen Basin glendonite data from Huggett et al. (2005).

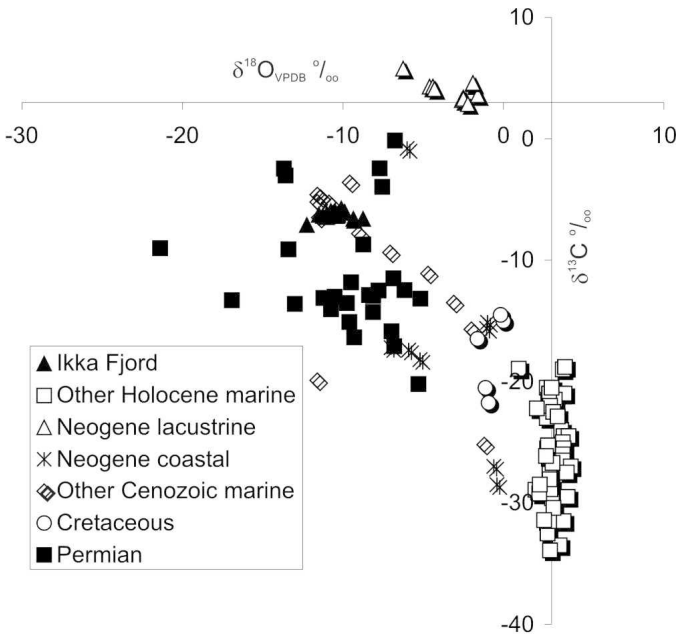

FIG. 6.—Stable-isotope data plot of glendonite calcite and ikaite (see Table 2 for sources of published data from localities noted). Other Holocene marine includes data from Bransfield Strait, Nankai Trough, Zaire Fan, Sea of Okhotsk; Neogene lacustrine includes data from Mono Lake, Pyramid Lake, Alkali Lake; Neogene coastal includes data from River Tyne, Hokkaido Island, Arctic Canada, Kola Peninsula; other Cenozoic marine includes data from Spitzbergen, Olympic Peninsula, Astoria, and Denmark; Permian includes data from Sydney, Tasmania, and Bowen basins.

study of brachiopods by Korte et al. (2005). The modest spread of the data may suggest some recrystallization or replacement of portions of the shell by later diagenetic cement. These data, however, serve as a useful reference for other Permian carbonate phases examined and suggest that the seawater in the Sydney Basin during brachiopod shell growth was near normal marine in terms of $\delta^{18}O$.

The calcite spar samples have very disparate isotopic compositions (Table 1; Fig. 5), with one exhibiting the most negative $\delta^{18}O$ signature (−24.2‰) of all the samples utilized in the present study, suggesting an elevated temperature of precipitation, or precipitation from isotopically light meteoric waters, or both. The former interpretation is preferred, given that this sample was collected from ~ 5 m below a Permian basalt flow and is likely related to the hydrothermal convective cell associated with the emplacement of this flow (Carr et al. 1999). The other spar sample is less negative in $\delta^{18}O$ and more typical of carbonate precipitated from meteoric waters. The two coalified wood samples analyzed in the current study have $\delta^{13}C$ values of ~ −22‰ and, if these are representative of Permian organic material in the early diagenetic system, carbonate ion derived from this material by direct oxidation to CO_2 and subsequent hydrolysis to produce carbonate would have $\delta^{13}C$ values of ~ −10‰.

The various Permian glendonite bulk samples, particularly those from the Sydney Basin, form a broad array in terms of their $\delta^{13}C$ and $\delta^{18}O$ values (Fig. 5). All of the Tasmania Basin samples have $\delta^{18}O$ values near −7‰, but the $\delta^{13}C$ data define two groups with values near 0‰ and −10‰, with the former group possibly indicating a physical mixture with biogenic calcite or the presence of early marine cements with heavier $\delta^{13}C$.

The separated amber and clear calcite are presumed to represent the primary calcite formed during the early conversion of ikaite to calcite (cf. Greinert and Derkachev 2004), and later infilling of pores respectively. Contrary to expectation, the clear and amber calcite separates do not form end members for simple mixing to produce the bulk glendonite in the three samples where all three components have been analyzed (Table 1; samples KP-7b, WH-4, and WH-7). Bulk glendonite and clear and amber calcite from the Sydney Basin show complete overlap in terms of their stable-isotope compositions suggesting that the scale of intergrowth of primary calcite and later spar is much finer than the millimeter-scale fragments that were separated by hand-picking.

All of the glendonite material, hand-picked separates and bulk, are lighter in $\delta^{18}O$ than the brachiopod samples, suggesting physical mixing of an isotopically lighter phase analogous to the late spar cement. Alternatively, the absence of any glendonite $\delta^{18}O$ values heavier than −5‰ may indicate initial precipitation from relatively lighter, mixed meteoric seawater sources during the ikaite phase.

The stable-isotope values of the additional samples of glendonite and related materials are presented in Table 1. The bivalve shell attached to the concretionary portion of one Kola Peninsula sample (MG-2a) has an isotopic signature consistent with precipitation of coeval, biogenic calcite. The shell has a heavier $\delta^{13}C$ signature than the associated glendonite samples, suggesting that methane-derived carbonate was involved in ikaite precipitation at that locality. While these glendonite samples apparently contain very little secondary calcite cement, minor amounts precipitated after transformation could also contribute to the isotopic signature.

The two nonmarine samples analyzed (Pyramid Lake and Alkali Lake; Table 1; Fig. 6) show no evidence of contribution of carbonate from methane, and the $\delta^{18}O$ signatures are controlled by the composition of the local meteoric waters. In addition, recrystallization of ikaite to calcite probably involved some additional precipitation of calcite cement crusts (tufas) with the $\delta^{18}O$ signature becoming heavier due to input from evaporated meteoric waters (cf. Benson 1994).

Results of Previous Studies

As shown in Figure 6, the stable-isotope signatures of modern glendonite and transformed ikaite (i.e., samples of ikaite that recrystallized to calcite during or after sampling. See references for details.)

illustrate distinctive trends, depending on the facies and mode of formation. Carbonate that crystallized displacively within the marine sediment pile in the Sea of Okhotsk, Zaire Fan, Nankai Trough, and Bransfield Strait has a narrow range of $\delta^{18}O$ values (mean +2.92‰; σ = 0.62‰; n = 49), suggesting precipitation from normal marine waters at temperatures consistent with the stability field of ikaite. The broader range of $\delta^{13}C$ values (mean −25.36‰; σ = 4.13‰; n = 49) is consistent with mixing of lighter carbonate from methane oxidation with heavier seawater carbonate.

Published $\delta^{18}O$ data for nonmarine transformed ikaite from Mono Lake are very similar to the values determined in the current study for samples from Pyramid Lake and Alkali Lake (Fig. 6). Ikaite formed during evaporation of the Hokkaido terrestrial spring has a $\delta^{18}O$ signature similar to that of samples from these three lakes, but the $\delta^{13}C$ signature for the spring is lighter. All of these terrestrial samples lack evidence for contribution of carbonate from methane, and the $\delta^{18}O$ signatures are controlled by the composition of the local meteoric waters.

Samples of transformed ikaite from Ikka Fjord have $\delta^{18}O$ values ranging from −8.78 to −12.25‰ resulting from precipitation from waters formed by mixing of meteoric, submarine spring water with seawater (Buchardt et al. 2001). The restricted and relatively heavy $\delta^{13}C$ signature (mean = 6.29‰; σ = 0.32‰; n = 19) suggests less significant contribution of carbonate ion from oxidized methane. Glendonite samples from the Neogene Hoh Formation subduction complex, Olympic Peninsula, Washington, have a very restricted range of isotopic values that overlap the lighter end of the spectrum for Ikka Fjord transformed ikaite (Fig. 6) and either have a meteoric input or a recrystallization event that homogenized their isotopic signature. The four analyzed glendonites from the marine, Miocene Astoria (Oregon) sequences show considerable scatter reflecting the variable input from meteoric water and recrystallization (Boggs 1972).

The Cretaceous Eromanga Basin (Australia) samples have $\delta^{18}O$ values similar to those of samples from the Kola Peninsula, Denmark, and the River Tyne (Fig. 6), and all are lighter in $\delta^{18}O$ than the modern, displacively grown glendonite and transformed ikaite materials. These Eromanga Basin materials were carefully studied using cathodoluminescence to assure that minimal non-glendonite material was included in the analyzed sample (De Lurio and Frakes 1999). If these materials represent pure, primary calcite from ikaite transformation, the isotopic data thus would suggest precipitation from Cretaceous seawater significantly lighter in $\delta^{18}O$ than modern seawater. We would expect that global seawater in the Cretaceous would have been lighter in $\delta^{18}O$ compared to the modern, due to absence of major continental glaciers. However, this is difficult to assess on the basis of the Cretaceous Eromanga Basin glendonite data, given the absence of data for biogenic carbonate from the same strata that host the glendonites. Biogenic calcite from elsewhere in the Eromanga Basin has $\delta^{18}O$ of 0.0 to +1.0‰, suggesting that locally the isotopic composition of waters was near modern seawater $\delta^{18}O$ (De Lurio and Frakes 1999). The lighter $\delta^{18}O$ signatures of glendonites from the Cretaceous Eromanga Basin could also be due to precipitation from waters with some meteoric contribution, like Ikka Fjord. Alternatively, the lighter $\delta^{18}O$ signature could signal admixture of minor, undetected diagenetic calcite cement. The light $\delta^{13}C$ signatures of the Denmark and River Tyne samples imply mixing between carbonate from methane oxidation and seawater carbonate.

Published isotope data for the Tertiary Spitzbergen and Recent Arctic Canada glendonites define fields intermediate between those for modern, marine, displacively grown ikaite and ikaite produced by mixing spring and seawater. The moderate scatter probably reflects recrystallization (Fig. 6). Stable-isotope data for three glendonite samples from the Late Permian Black Alley Shale of the Bowen Basin, eastern Australia (Huggett et al. 2005), all plot within the field defined by glendonites from the contiguous Sydney Basin and the coeval Tasmania Basin (Fig. 6).

DISCUSSION

Glendonites in the Sydney Basin are commonly associated with facies containing unequivocal evidence for ice rafting and episodically cold climate systems (Thomas et al. 2005). This, together with the stability of ikaite, indicates that glendonites are undoubtedly proxies for cold water conditions (< 4°C). The occurrence of ikaite in the Zaire Fan indicates, however, that their recognition cannot be taken as evidence for high palaeolatitudes unless they come from recognized continental shelf or non-marine deposits that show no evidence of upwelling.

The random orientation of long axes, coupled with the partial or complete enclosure of fossils or pebbles, indicate that the glendonites developed within the sediment pile rather than at the water–sediment interface. Sedimentary layers containing abundant rounded dropstones likely record times of greatest ice influence in the Sydney Basin. The rounded nature of these erratics indicates that they were derived from sea or river ice, and not icebergs as suggested by Eyles et al. (1998), because the latter would have deposited angular erratics. The relative scarcity of dropstones and shelly fossils in glendonite-bearing beds may represent slow (sediment starved) deposition in deeper water at a greater distance from the coast during periods of maximum forced transgression. Early uplift offshore caused by the passing of the initial subduction bulge may have induced thermocline stratification within the water column, promoting ikaite deposition. In such circumstances, sedimentation rates are reduced, detritus grain size is diminished, and ikaite precipitates from the cold porewater to grow displacively in the sediment pile. Alternatively, because most of the ikaite-bearing horizons are overlain by coarser sediment containing many dropstones, they may be preserved within the finer underlying sediment during the regressive phases of smaller-scale parasequences when sea level fell and the climate would have been substantially colder.

Stable-isotope values for Permian samples from the Sydney, Bowen, and Tasmania basins of eastern Australia, including the separated amber "primary" calcite and "secondary" white calcite cement, define a broad range. This suggests that these Permian glendonites do not reliably record stable-isotope chemistry of the waters in which the ikaite originally formed, at least at the scale of our sampling and subsampling. The $\delta^{18}O$ data for these glendonites are best interpreted as resulting from mixtures of relatively heavier "primary" calcite from ikaite transformation with relatively lighter calcite that precipitated at elevated temperatures during burial diagenesis. Both types of calcite are clearly observed in thin-section, but hand-picked separation of millimeter-scale fragments was not sufficient to provide distinctive stable-isotope data.

The $\delta^{18}O$ data for the Permian glendonites can also be interpreted as homogenization of the isotope signatures during later burial at elevated temperatures by recrystallization of the "primary" amber calcite coincident with precipitation of the burial cement. Such recrystallization, however, is expected to result in relatively homogeneous $\delta^{18}O$ values, rather than the broad range of values observed. Another possibility that cannot be discounted is that some of the Permian glendonites were precipitated from fluids that had a modest contribution of isotopically lighter meteoric water. Sandy facies underlying some of the glendonite-bearing units could have served as submarine aquifers that transported isotopically light water into the shelf strata, where it emerged, as at Ikka Fjord, as submarine springs. While the stable-isotope signature of brachiopods from the Sydney Basin strata suggest normal marine waters during their growth, the meltwater from sea-ice or river-ice contribution to the ambient seawater could have locally influenced the $\delta^{18}O$ of precipitated ikaite. Brachiopods possibly grew during periods of normal marine salinity whereas ikaite formed later by displacive growth in sediment whose porewaters were diluted by meltwater.

The $\delta^{13}C$ data for the Permian glendonites show a wide range of values (~ 0 to −20‰) that are best explained as a mixture of depleted carbonate derived from methane oxidation mixed with heavier, seawater-derived

carbonate. Brachiopod shells from the Sydney Basin have $\delta^{13}C$ values consistent with derivation of carbonate from a normal marine, well-mixed water column. The intermediate $\delta^{13}C$ of the Sydney Basin spar likewise represents mixing of carbonate from biogenic calcite or aragonite dissolution and carbonate from an organic source. The $\sim -22‰$ $\delta^{13}C$ of the organic carbon from coalified wood in the Sydney Basin indicates that carbonate with $\sim -10‰$ $\delta^{13}C$ could be derived by direct oxidation of this terrestrial organic matter, so that late spar cement need not involve oxidation of methane to produce the observed isotopic composition.

CONCLUSIONS

Pseudomorphic replacements of ikaite by calcite (glendonites) are relatively common in the rock record in association with coldwater sedimentary facies. The distribution of modern ikaite is controlled by water temperature and pressure, and precipitation is favored by elevated alkalinity and dissolved phosphate. These conditions are found in a wide range of environments from deep marine to lacustrine settings.

Glendonites from the Permian Sydney Basin formed in organic-rich marine shelf sediment. The distribution of glendonites in Sydney Basin strata is consistent with a cold-water origin.

Stable-isotope data from modern ikaite and Holocene glendonite suggest that ikaite precipitates in equilibrium with ambient water and that carbonate is often derived from oxidation of methane.

Stable-isotope data from ancient glendonites, including Sydney Basin samples, indicate that precipitation of late diagenetic cement and possible recrystallization of "primary" glendonite calcite may obscure the original isotopic signature. Refined microscale sampling may be required to differentiate early calcite replacement of ikaite from later-burial diagenetic calcite Ancient glendonites may have value as recorders of the isotopic character of the waters from which the primary ikaite precipitated if primary carbonate signatures can be extracted.

ACKNOWLEDGMENTS

We are indebted to the curators of the Smithsonian Institution for supply of the Pyramid Lake specimen, and Ralf Botrill (Tasmanian Department of Mines) for supply of Tasmania Basin samples. We also appreciate advice of Stephen Howe, State University of New York at Albany, regarding sample preparation for stable isotope analyses. BWS acknowledges the Malcolm and Sylvia Boyce Fund at Colgate University for support of analytical costs. BGJ and PFC acknowledge support from the GeoQuEST Research Centre at the University of Wollongong. The thoughtful and thorough reviews of the manuscript by Eugene Domack and Tracy L. Franks are gratefully acknowledged, and the careful editorial assistance of John B. Southard is greatly appreciated.

REFERENCES

Auclair, A.C., Joachimski, M.M., and Lecuyer, C., 2003, Deciphering kinetic, metabolic and environmental controls on stable isotope fractionations between seawater and the shell of *Terebratalia transversa* (Brachiopoda): Chemical Geology, v. 202, p. 59–78.

Benson, L., 1994, Carbonate deposition, Pyramid Lake Subbasin, Nevada: 1. Sequence of formation and elevational distribution of carbonate deposits (tufas): Palaeogeography, Palaeoclimatology, Palaeoecology, v. 109, p. 55–87.

Bischoff, J.L., Fitzpatrick, J.A., and Rosenbauer, R.J., 1993a, The solubility and stabilization of ikaite ($CaCO_3{\cdot}6H_2O$) from 0° to 25°C; environmental and paleoclimatic implications for thinolite tufa: Journal of Geology, v. 101, p. 21–33.

Bischoff, J.L., Stine, S., Rosenbauer, R.J., Fitzpatrick, J.A., and Stafford, T.W, Jr, 1993b, Ikaite precipitation by mixing of shoreline springs and lake water, Mono Lake, California, USA: Geochimica et Cosmochimica Acta, v. 57, p. 3855–3865.

Boggs, S., 1972, Petrography and geochemistry of rhombic, calcite pseudomorphs from mid-Tertiary mudstones of the Pacific Northwest, U.S.A.: Sedimentology, v. 19, p. 219–235.

Bradshaw, M.T., Brakel, A.T., Parrish, J.T., Totterdell, J.M., and Yeates, A.N., 1995, Paleoclimatology of Australia during the Pangaean interval (abstract): SEPM and American Association of Petroleum Geologists, Annual Meeting Abstracts, v. 4, 12 p.

Brand, U., 2004, Carbon, oxygen and strontium isotopes in Paleozoic carbonate components: an evaluation of original seawater-chemistry proxies: Chemical Geology, v. 204, p. 23–44.

Brandley, R.T., and Krause, F.F., 1994, Thinolite-type pseudomorphs after ikaite: indicators of cold water on the subequatorial western margin of Lower Carboniferous North America, *in* Beauchamp, B., Embry, A.F., and Glass, D., eds., Pangea: Global Environments and Resources: Canadian Society of Petroleum Geologists, Memoir 17, p. 333–344.

Brandt, K., 1986, Glacioeustatic cycles in the Early Jurassic?: Neues Jahrbuch für Geologie und Palaontologie, Monatshefte, v. 5, p. 257–274.

Buchardt, B., Seaman, P., Lindal, E., Stockmann, G., Vous, M., and Wilken, U., 1998, Ikaite from the type locality in South Greenland: formation of an unstable, low-temperature carbonate: Nordic Geological Winter Meeting, Abstracts, v. 23, 43 p.

Buchardt, B., Israelson, C., Seaman, P., and Stockmann, G., 2001, Ikaite tufa towers in Ikka Fjord, Southwest Greenland: their formation by mixing of seawater and alkaline spring water: Journal of Sedimentary Research, v. 71, p. 176–189.

Carr, P.F., Jones, B.G., and Middleton, R.G., 1989, Precursor and formation of glendonites in the Sydney Basin: Australian Mineralogist, v. 4, p. 3–12.

Carr, P.F., Pemberton, J.W., and Nunan, E., 1999, Low grade metamorphism of mafic lavas, Late Permian Broughton Formation, Sydney Basin: Australian Journal of Earth Sciences, v. 46, p. 839–849.

Council, T.C., and Bennett, P.C., 1993, Geochemistry of ikaite formation at Mono Lake, California: implications for the origin of tufa mounds: Geology, v. 21, p. 971–974.

Dana, E.S., 1884, A crystallographic study of the thinolite of Lake Lahontan: U.S. Geological Survey, Bulletin 12, p. 429–450.

Dana, J.D., 1849, United States Exploring Expedition. During the years 1838, 1839, 1840, 1841, 1842. Under the command of Charles Wilkes, U.S.N., v. X, Geology: Philadelphia, C. Sherman.

David, T.W.E., Taylor, T.G., Woolnough, W.G., and Foxall, H.G., 1905, Occurrence of the pseudomorph glendonites in New South Wales: Geological Survey of New South Wales, Records, v. 8, p. 162–179.

De Lurio, J.L., and Frakes, L.A., 1999, Glendonites as a paleoenvironmental tool: implications for Early Cretaceous high latitude climates in Australia: Geochimica et Cosmochimica Acta, v. 63, p. 1039–1048.

Dickens, J.M., 1996, Problems of a Late Palaeozoic glaciation in Australia and subsequent climate in the Permian: Palaeogeography, Palaeoclimatology, Palaeoecology, v. 125, p. 185–197.

Domack, E.W., Collins, S., Burrett, C., and Bendall, M., 1998, Geochemical stratigraphy of a late Paleozoic glacialmarine mudstone of the Tasmania Basin: glendonites, oil shales, and paleoproductivity (abstract): Geological Society of America, Abstracts with Programs, v. 30, n. 7, 337 p.

Eyles, C.H., and Eyles, N., 2000, Subaqueous mass flow origin for Lower Permian diamictites and associated facies of the Grant Group, Barbwire Terrace, Canning Basin, Western Australia: Sedimentology, v. 47, p. 343–356.

Eyles, C.H., Eyles, N., and Gostin, V.A., 1998, Facies and allostratigraphy of high-latitude, glacially influenced marine strata of the Early Permian southern Sydney Basin, Australia: Sedimentology, v. 45, p. 121–162.

Fielding, C.R., Sliwa, R., Holcombe, R.J., and Jones, A.T., 2001, A new palaeogeographic synthesis for the Bowen, Gunnedah and Sydney Basins of eastern Australia, *in* Hill, K.C., and Bernecker, T., eds., Eastern Australasian Basins Symposium 2001: A Refocused Energy Perspective for the Future: Petroleum Exploration Society of Australia, Special Publication, p. 269–278.

Fielding, C.R., Bann, K.L., MacEachern, J.A., Tye, S.C., and Jones, B.G., 2006, Cyclicity in the nearshore marine to coastal, Lower Permian Pebbley Beach Formation, southern Sydney Basin, Australia: a record of relative sea-level fluctuations at the close of the Late Palaeozoic Gondwanan ice age: Sedimentology, v. 53, p. 435–463.

Francis, J.E., and Frakes, L.A., 1988, Early Cretaceous high-latitude cold climates; implications for Cretaceous polar biotas (abstract): Palaeontological Association, Aston Annual Conference, Abstracts, v. 5.

Gostin, V.A., and Herbert, C., 1973, Stratigraphy of the Upper Carboniferous and Lower Permian sequence, southern Sydney Basin: Geological Society of Australia, Journal, v. 20, p. 49–70.

Greinert, J., and Derkachev, A., 2004, Glendonites and methane-derived Mg-calcites in the Sea of Okhotsk, eastern Siberia: implications of a venting-related ikaite/glendonite formation: Marine Geology, v. 204, p. 129–144.

Herbert, C., 1995, Sequence stratigraphy of the Late Permian coal measures in the Sydney Basin: Australian Journal of Earth Sciences, v. 42, p. 391–405.

Huggett, J.M., Schultz, B.P., Shearman, D.J., and Smith, A.J., 2005, The petrology of ikaite pseudomorphs and their diagenesis: Proceedings of the Geologist's Association, v. 116, p. 207–220.

Isbell, J.L., Miller, M.F., Wolfe, K.L., and Lenaker, P.A., 2003, Timing of Late Paleozoic glaciation in Gondwana: was glaciation responsible for the development of northern hemisphere cyclothems? *in* Chan, M.A., and Archer, A.W., eds., Extreme Depositional Environments: Mega End Members in Geologic Time: Geological Society of America, Special Paper 370, p. 5–24.

Ito, T., 1996, Ikaite from cold spring water at Shiowakka, Hokkaido, Japan: Journal of Mineralogy, Petrology and Economic Geology, v. 91, p. 209–219.

Ito, T., 1998, Factors controlling the transformation of natural ikaite from Shiowakka, Japan: Geochemical Journal, v. 32, p. 267–273.

Ito, T., Matsubara, S., and Miyawaki, R., 1999, Vaterite after ikaite in carbonate sediment: Journal of Mineralogy, Petrology and Economic Geology, v. 94, p. 176–182.

James, N.P., Narbonne, G.M., Dalrymple, R.W., and Kyser, T.K., 2005, Glendonites in Neoproterozoic low-latitude, interglacial sedimentary rocks, northwest Canada: insights into the Cryogenian ocean and Precambrian cold-water carbonates: Geology, v. 33, p. 9–12.

Jansen, J.H.F., Woensdregt, C.F., Kooistra, M.J., and van der Gaast, S.J., 1987, Ikaite pseudomorphs in the Zaire deep-sea fan: an intermediate between calcite and porous calcite: Geology, v. 15, p. 245–248.

Johnston, J.D., 1995, Pseudomorphs after ikaite in a glaciomarine sequence in the Dalradian of Donegal, Ireland: Scottish Journal of Geology, v. 31, p. 3–9.

Jones, A.T., and Fielding, C.R., 2004, Sedimentological record of the Late Paleozoic glaciation in Queensland, Australia: Geology, v. 32, p. 153–156.

Kaplan, M.E., 1979, Calcite pseudomorphs (pseudogaylussite, jarrowite, thinolite, glendonite, gennoishi, White Sea hornlets) in sedimentary rocks: origins of the pseudomorphs: Lithology and Mineral Resources, v. 14, p. 623–636.

Kennedy, G.L., Hopkins, D.M., and Pickthorn, W.J., 1987, Ikaite, the glendonite precursor, in estuarine sediments at Barrow, Arctic Alaska (abstract): Geological Society of America, Abstracts with Programs, v. 19, 725 p.

Kodina, L.A., Tokarev, V.G., Vlasova, L.N., Bychkov, A.M., and Mardanjan, I.Y., 2002, New findings of ikaite in the Kara Sea during R/V "Akademik Boris Petrov" Cruise 36, September 2001: Reports on Polar and Marine Research, v. 419, p. 164–172.

Kodina, L.A., Tokarev, V.G., Vlasova, L.N., and Korobeinik, G.S., 2003, Contribution of biogenic methane to ikaite formation in the Kara Sea; evidence from the stable carbon isotope geochemistry: Proceedings in Marine Science, v. 6, p. 349–374.

Koenigsberger, E., Koenigsberger, L.C., and Gamsjaeger, H., 1999, Low-temperature thermodynamic model for the system Na_2CO_3–$MgCO_3$–$CaCO_3$–H_2O: Geochimica et Cosmochimica Acta, v. 63, p. 3105–3119.

Korte, C., Kozur, H.W., and Veizer, J., 2005, $\delta^{13}C$ and $\delta^{18}O$ values of Triassic brachiopods and carbonate rocks as proxies for coeval seawater and palaeotemperature: Palaeogeography, Palaeoclimatology, Palaeoecology, v. 226, p. 287–306.

Le Roux, J.P., and Jones, B.G., 1994, Lithostratigraphy and depositional environment of the Nowra Sandstone in the southwestern Sydney Basin, Australia: Australian Journal of Earth Sciences, v. 41, p. 191–203.

Lennie, A.R., Tang, C.C., and Thompson, S.P., 2004, The structure and thermal expansion behaviour of ikaite $CaCO_3{\cdot}6H_2O$ from T = 114 to T = 293°K: Mineralogical Magazine, v. 68, p. 135–146.

Marland, G., 1975, The stability of $CaCO_3{\cdot}6H_2O$ (ikaite): Geochimica et Cosmochimica Acta, v. 39, p. 83–91.

Mikkelsen, A., Anderson, A.B., Engelsen, S.B., Hansen, H.C., Larsen, O., and Skibsted, L.H., 1999, Presence and dehydration of ikaite, calcium carbonate hexahydrate, in frozen shrimp shell: Journal of Agricultural and Food Chemistry, v. 47, p. 911–917.

Pauly, H., 1963, "ikaite," a new mineral from Greenland: Arctic, v. 16, p. 263–264.

Rickaby, R.E.M., Shaw, S., Bennitt, G., Kennedy, H., Zabel, M., and Lennie, A., 2006, Potential of ikaite to record evolution of oceanic $\delta^{18}O$: Geology, v. 34, p. 497–500.

Schubert, C.J., Nurnberg, D., Scheele, N., Pauer, F., and Kriews, M., 1997, ^{13}C isotope depletion in ikaite crystals: evidence for methane release from the Siberian shelves?: Geo-Marine Letters, v. 17, p. 169–174.

Shaikh, A.M., and Shearman, D.J., 1987, On ikaite and the morphology of its pseudomorphs, *in* Rodriguez-Clemente, R., and Tardy, Y., eds., Geochemistry and Mineral Formation in the Earth Surface: International Meeting on Geochemistry of the Earth and Processes of Mineral Formation, p. 791–803.

Sheard, M.J., 1990, Glendonites from the southern Eromanga Basin in South Australia: palaeoclimatic indicators for Cretaceous ice: Geological Survey of South Australia, Quarterly Geological Notes, v. 114, p. 17–21.

Shearman, D., 1998, The Mono Lake tufas and ikaite columns of Ikka Fjord, Greenland: Geoscientist, v. 8, p. 4–5.

Shearman, D., and Smith, A.J., 1985, Ikaite, the parent mineral of jarrowite-type pseudomorphs: Proceedings of the Geologist's Association, v. 96, p. 305–314.

Shi, G.R., 2001, Possible influence of Gondwanan glaciation on low-latitude carbonate sedimentation and trans-equatorial faunal migration: the Lower Permian of South China: Geosciences Journal, v. 5, p. 57–63.

Socki, R.A., Gibson, E.K., Golden, D.C., Ming, D.W., and McKay, A., 2003, Kinetic fractionation of stable isotopes in carbonates on Mars: terrestrial analogues (abstract): Lunar and Planetary Science XXXIV, Abstract 1938.

Stein, C.L., and Smith, A.J., 1986, Authigenic carbonate nodules in the Nankai Trough, Site 583: Initial Reports of the Deep Sea Drilling Project, v. 87, p. 659–668.

Suess, E., Balzer, W., Hesse, K.F., Mueller, P.J., Ungerer, C.A., and Wefer, G., 1982, Calcium carbonate hexahydrate from organic-rich sediments of the Antarctic shelf; precursors of glendonites: Science, v. 216, p. 1128–1131.

Swainson, I.P., and Hammond, R.P., 2001, Ikaite, $CaCO_3{\cdot}6H_2O$: cold comfort for glendonites as paleothermometers: American Mineralogist, v. 86, p. 1530–1533.

Thomas, S.G., Frank, T.D., and Fielding, C., 2005, Glendonites as paleoclimate indicators within the Middle Permian Wandrawandian Siltstone, southern Sydney Basin, Australia (abstract): Geological Society of America, Abstracts with Programs, v. 36, no. 5, 16 p.

Tye, S.C., Fielding, C.R., and Jones, B.G., 1996, Stratigraphy and sedimentology of the Permian Talaterang and Shoalhaven groups in the southernmost Sydney Basin, New South Wales: Australian Journal of Earth Sciences, v. 43, p. 57–69.

Veizer, J., Ala, D., Karem, A., Bruckschen, P., Buhl, D., Bruhn, F., Carden, G., Diener, A., Ebneth, S., Godderis, Y., Jasper, T., Korte, C., Pawellek, F., Podlaha, O., and Strauss, H., 1999, $^{87}Sr/^{86}Sr$, $\delta^{13}C$ and $\delta^{18}O$ evolution of Phanerozoic seawater: Chemical Geology, v. 161, p. 59–88.

Whiticar, M.J., and Suess, E., 1998, The cold carbonate connection between Mono Lake, California and the Bransfield Strait, Antarctica: Aquatic Geochemistry, v. 4, p. 429–454.

Yan, J., 1996, Ikaite pseudomorphs, cold water indicators in the Chihsia Formation (Early Permian) of South China (abstract): 30th International Geological Congress, Abstracts, v. 30, 97 p.

Zabel, M., and Schulz, H.D., 2001, Importance of submarine landslides for non-steady state conditions in pore water systems; lower Zaire (Congo) deep-sea fan: Marine Geology, v. 176, p. 87–99.

Received 18 January 2006; accepted 8 June 2007.